

DEVELOPING D-OPTIMUM EXPERIMENTAL CONDITIONS FOR MODEL-BASED FAULT DETECTION SYSTEMS

Marcin Witczak *

* *Institute of Control and Computation Engineering,
University of Zielona Góra,
ul. Podgórna 50, 65-246 Zielona Góra, Poland,
e-mail: M.Witczak@issi.uz.zgora.pl*

Abstract: The main objective of this paper is to show an importance of developing suitable experimental conditions while designing and utilizing model-based fault detection systems. In particular, the paper shows the possibilities of exploiting the theory of optimum experimental design in parameter-estimation-based fault detection schemes. More precisely, a novel scheme for measuring and diagnosing an impedance is proposed. *Copyright©2005 IFAC.*

Keywords: parameter estimation, non-linear systems, experimental design, fault diagnosis, fault detection

1. INTRODUCTION

A fault detection process (Chen and Patton, 1999; Korbicz *et al.*, 2004; Witczak, 2003) can be perceived as a two-stage procedure, i.e. residuals generation and symptom evaluation based on these residuals. The residual can be defined in many different ways depending on the choice of the fault diagnosis scheme, e.g. in the parameter-estimation-based scheme the residual is defined as a difference between the nominal and estimated values of the parameters while in most of the schemes the residual is perceived as difference between the output of the model and that of the system. The residual should ideally carry an information regarding a fault only. Under such an assumption, the faults can be detected by setting a fixed threshold on the residual. The fundamental difficulty with this kind of symptom evaluation is that the residuals are normally uncertain, corrupted by noise, disturbances and modelling uncertainty. That is why it is necessary to assign a threshold (significantly) larger than zero in order to avoid false alarms. This usually

implies a reduction of fault detection sensitivity. Thus, threshold selection should be performed in such a way so as to attain a compromise between the fault detection sensitivity and the false-alarm rate. An obvious remedy to the above mentioned problems is to utilize the knowledge regarding model uncertainty. One of the possible approaches to gather such knowledge is to use statistical techniques (Atkinson and Donev, 1992; Uciński, 2005; Walter and Pronzato, 1997) to obtain parametric uncertainty of the model. This knowledge makes it possible to design the so-called adaptive threshold (Frank *et al.*, 1999) that allows robust fault detection. Apart from the possibilities of generating an adaptive threshold, the knowledge regarding model uncertainty makes it possible to formulate suitable criteria of the optimum experimental design (OED) (Atkinson and Donev, 1992; Uciński, 2005; Walter and Pronzato, 1997) that allow minimization of model uncertainty. This means that more accurate models can be obtained resulting in an increase of fault sensitivity as well as an increase in a general relia-

bility of the fault diagnosis scheme. Another kind of solutions that may increase the performance of the fault diagnosis scheme is based on an appropriate scheduling of the control test signals in such a way so as to gain as much information as possible about the system being supervised (Delebecque *et al.*, 2003).

The paper shows the possibilities of exploiting the theory of OED in parameter-estimation-based fault detection schemes. The paper is organized as follows. In the second section, a novel scheme for measuring and diagnosing an impedance is proposed. The final part of the paper is devoted to the numerical simulations and conclusions.

2. IMPEDANCE MEASUREMENT AND DIAGNOSIS

The objective of this section is to propose a new impedance measurement and diagnosis scheme. The idea of measuring the impedance with the so-called virtual bridge was introduced by (Dutta *et al.*, 1987). The virtual bridge is composed of two arms, namely a real (hardware) arm, as shown in Fig. 1 and a virtual arm that is implemented with the help of a computer. Dutta *et al.* (1987) formulated the problem of balancing the bridge as a non-linear parameter estimation one. To solve such a problem they employed the gradient descent algorithm. Other researchers (Awad *et al.*, 1994) developed some modifications of the algorithm proposed in (Dutta *et al.*, 1987) that increased its convergence. Unfortunately, none of the authors has provided an analytical rules for estimating the accuracy of the obtained impedance, i.e. knowledge about model uncertainty. Moreover, they have not provided any analytical rules that can be used for obtaining an auxiliary resistance R_r and the sampling time. Another question that arises while analysing (Dutta *et al.*, 1987; Awad *et al.*, 1994; Angrisani *et al.*, 1996) is as follows: Is this really necessary to use the non-linear parameter estimation techniques for estimating R and C ? First, let us observe that for the scheme

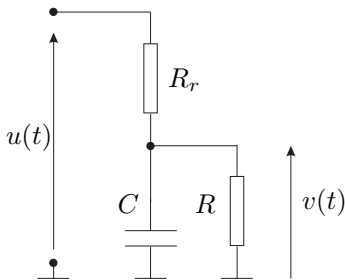


Fig. 1. An impedance measurement scheme

presented in Fig. 1 the following current equality can be established:

$$C \frac{dv(t)}{dt} + \frac{v(t)}{R} = \frac{u(t) - v(t)}{R_r}, \quad (1)$$

Assuming that $u(t) = U\sqrt{2}\sin(\omega t)$, the steady-state solution of (1) can be written as:

$$v(t) = \rho U \sqrt{2} R ((R + R_r) \sin(\omega t) - R_r R C \omega \cos(\omega t)), \quad (2)$$

where $\rho = (R^2 + 2R_r R + R_r^2(1 + \omega^2 R^2 C^2))^{-1}$. Equation (2) can be transformed into a discrete-time form and written as follows:

$$v_k = p_1 u_{1,k} + p_2 u_{2,k}, \quad (3)$$

where

$$p_1 = \rho R (R + R_r), \quad p_2 = \rho R_r C \omega R^2, \quad (4)$$

and $u_{1,k} = U\sqrt{2}\sin(\omega k\tau)$, $u_{2,k} = U\sqrt{2}\cos(\omega k\tau)$ where τ stands for the sampling time. In this paper it is assumed that $u_{1,k}$ and $u_{2,k}$ are available. This is a mild assumption since it is not difficult to design a hardware providing such signals. Another important fact that can be observed while analysing (3) is that it can be perceived as a linear-in-parameter model with respect to p_1 and p_2 . Contrary to (Dutta *et al.*, 1987; Awad *et al.*, 1994) where the non-linear parameter estimation techniques were employed for obtaining R and C , it is proposed to use the classical recursive least-square (RLS) algorithm for estimation of p_1 and p_2 . Such an algorithm can be given as follows:

$$\hat{\mathbf{p}}_{k+1} = \hat{\mathbf{p}}_k + \mathbf{k}_{k+1} \varepsilon_{k+1}, \quad (5)$$

$$\mathbf{k}_{k+1} = \mathbf{P}_k \mathbf{r}_{k+1} (1 + \mathbf{r}_{k+1}^T \mathbf{P}_k \mathbf{r}_{k+1})^{-1}, \quad (6)$$

$$\varepsilon_{k+1} = y_{k+1} - f(\hat{\mathbf{p}}_k, \mathbf{u}_{k+1}), \quad (7)$$

$$\mathbf{P}_{k+1} = [\mathbf{I}_{n_p} - \mathbf{k}_{k+1} \mathbf{r}_{k+1}^T] \mathbf{P}_k, \quad (8)$$

where stands for the so-called forgetting factor, y_k is the k -th measurement of v_k , $f(\hat{\mathbf{p}}_k, \mathbf{u}_{k+1}) = \hat{p}_{1,k} u_{1,k+1} + \hat{p}_{2,k} u_{2,k+1}$, $\mathbf{r}_k = [u_{1,k}, u_{2,k}]^T$, and $\hat{\mathbf{p}}_k = [\hat{p}_{1,k}, \hat{p}_{2,k}]^T \in \mathbb{R}^{n_p}$ denotes the k -th estimate of \mathbf{p} . Thus, knowing $\hat{\mathbf{p}}$ it is possible to obtain estimates of R and C according to the following equations:

$$\hat{R} = -\frac{R_r (\hat{p}_1^2 + \hat{p}_2^2)}{\hat{p}_1^2 + \hat{p}_2^2 - \hat{p}_1}, \quad (9)$$

$$\hat{C} = -\frac{\hat{p}_2}{R_r \omega (\hat{p}_1^2 + \hat{p}_2^2)}, \quad (10)$$

obtained by solving (4) with respect to R and C . It should be also pointed out that when there is no need for on-line estimation of the impedance then the classical, non-recursive least-square algorithm can be employed. The well-known advantage of this algorithm, comparing with its recursive counterpart, is that the highest estimation accuracy can be attained with a smaller n_t . In this case, estimates of p_1 and p_2 can be computed as follows:

$$\hat{p}_1 = \frac{\gamma_2 \eta - \beta_2 \gamma_1}{\eta^2 - \beta_1 \beta_2}, \quad \hat{p}_2 = \frac{\gamma_1 \eta - \beta_1 \gamma_2}{\eta^2 - \beta_1 \beta_2}, \quad (11)$$

where

$$\begin{aligned}\gamma_i &= \sum_{k=1}^{n_t} u_{i,k} y_k, & \eta &= \sum_{k=1}^{n_t} u_{1,k} u_{2,k}, \\ \beta_i &= \sum_{k=1}^{n_t} u_{i,k}^2.\end{aligned}\quad (12)$$

2.1 Initialization of the RLS algorithm

As can be found in the literature (Walter and Pronzato, 1997) regarding the RLS algorithm, the initial matrix \mathbf{P}_k , i.e. \mathbf{P}_0 should be set as $\mathbf{P}_0 = \gamma \mathbf{I}$ where γ stands for a sufficiently large positive constant (usually 10^3 – 10^{20}). When some rough values of R and C are known then $\hat{\mathbf{p}}_0$ should be initialized according to (4). Otherwise, it can be observed from (9) that $\hat{p}_1^2 + \hat{p}_2^2 - \hat{p}_1 < 0$ and hence:

$$\frac{1}{2} - \frac{1}{2} \sqrt{1 - 4\hat{p}_2^2} < \hat{p}_1 < \frac{1}{2} + \frac{1}{2} \sqrt{1 - 4\hat{p}_2^2}. \quad (13)$$

Since \hat{p}_2 should satisfy $1 - 4\hat{p}_2^2 > 0$ and (10) indicates that $\hat{p}_2 < 0$ then it is clear that:

$$-\frac{1}{2} < \hat{p}_2 < 0. \quad (14)$$

Thus, when no knowledge is available about R and C then $\hat{\mathbf{p}}_0$ should be set so as to satisfy (13)–(14).

2.2 Confidence region and fault detection

The solutions presented in the subsequent part of this paper are based on the following assumption:

$$y_k = v_k + \epsilon_k, \quad (15)$$

where ϵ stands for the zero-mean, uncorrelated, Gaussian noise sequence. In other words, ϵ represents the difference between the output of the model (3) and y_k that represents the actual measurements of v_k (cf. Fig. 1).

Since estimates of R and C are known, the next problem being considered is to obtain a set of all possible \hat{R} and \hat{C} that are consistent with the measurements. Such a set can easily be obtained with the use of $(1 - \alpha)100\%$ confidence region (Walter and Pronzato, 1997) for \mathbf{p} and equations (4). As a result the following inequality is given:

$$\mathbf{d}_k^T \mathbf{P}_k^{-1} \mathbf{d}_k \leq 2\hat{\sigma}_k^2 F_{\alpha,2,k-2} \quad (16)$$

where

$$\mathbf{d}_k = \hat{\mathbf{p}}_k - \rho [R(R + R_r), R_r C \omega R^2]^T, \quad (17)$$

and $F_{\alpha,2,k-2}$ stands for the F-Snedecor distribution quantile with 2 and $k - 2$ degrees of freedom, and $\hat{\sigma}$ is the estimate of the standard deviation.

Thus, the problem of fault detection can be transformed into the task of testing the hypotheses. This means that, at the α -level, the hypothesis:

$$\begin{aligned}\mathcal{H}_0 &: (R, C) = (R_0, C_0) \\ \text{vs.} \\ \mathcal{H}_1 &: (R, C) \neq (R_0, C_0),\end{aligned}\quad (18)$$

where R_0, C_0 are the required values of R and C , is rejected when the inequality (16) is violated. The acceptance of hypothesis \mathcal{H}_1 denotes the faulty behaviour of the impedance.

2.3 Application of OED

As we can see from (16), the size of the confidence region depends on the so-called Fisher Information Matrix (FIM) \mathbf{P}^{-1} . On the other hand, FIM depends on the experimental conditions, e.g. $\xi = [\mathbf{u}_1, \dots, \mathbf{u}_{n_t}]$. Thus, optimal experimental conditions can be obtained by optimising some scalar function $\Phi(\mathbf{P}^{-1})$. Such a function can be defined in several different ways (Atkinson and Donev, 1992; Uciński, 2005; Walter and Pronzato, 1997). In this paper, the so called D-optimality criterion is used, i.e. $\Phi(\mathbf{P}^{-1}) = \det(\mathbf{P}^{-1})$ is maximised. It should be also pointed out that the experimental conditions are developed for R and C but not for p_1 and p_2 . This means that all dependencies among R_r, ω, τ, R , and C that provide additional source of knowledge are exploited. First, let us define FIM:

$$\mathbf{P}^{-1} = \sum_{k=1}^{n_t} \mathbf{r}_k \mathbf{r}_k^T, \quad \mathbf{r}_k = \left[\frac{\partial v_k}{\partial R}, \frac{\partial v_k}{\partial C} \right]^T, \quad (19)$$

The purpose of further consideration is to obtain D-optimum values of R_r and τ , i.e. R_r and τ that maximise $\det(\mathbf{P}_k^{-1})$.

It can be observed that:

$$\begin{aligned}\mathbf{r}_k &= \mathbf{P}_1 \mathbf{r}_{1,k}, & \mathbf{P}_1 &= \sqrt{2} U R_r \rho^2 \text{diag}(1, \omega R^2), \\ \mathbf{r}_{1,k} &= [a \sin(\omega k \tau) + b \cos(\omega k \tau), \\ & b \sin(\omega k \tau) - a \cos(\omega k \tau)] \\ a &= R^2 + 2R_r R + R_r^2 (1 - \omega^2 R^2 C^2), \\ b &= -2C\omega(R_r R^2 + R R_r^2).\end{aligned}$$

Bearing in mind that:

$$\begin{aligned}\sqrt{a^2 + b^2} \sin(\omega k \tau + \arctan(a/b)) \\ = a \sin(\omega k \tau) + b \cos(\omega k \tau), \\ \sqrt{a^2 + b^2} = \rho^{-1},\end{aligned}\quad (20)$$

it is possible to write:

$$\begin{aligned}\mathbf{r}_k &= \mathbf{P}_2 \mathbf{r}_{2,k}, & \mathbf{P}_2 &= \sqrt{2} U R_r \rho \text{diag}(1, \omega R^2), \\ \mathbf{r}_{2,k} &= [\sin(\omega k \tau + \arctan(a/b)), \\ & \sin(\omega k \tau + \arctan(-b/a))]^T.\end{aligned}\quad (21)$$

Using equations (21), now FIM can be given as follows:

$$\mathbf{P}^{-1} = \mathbf{P}_2 \sum_{k=1}^{n_t} \mathbf{r}_{2,k} \mathbf{r}_{2,k}^T \mathbf{P}_2 \quad (22)$$

The main difficulty associated with further consideration is concerned with the selection of the number of measurements n_t . Indeed, it is very difficult to give n_t *a priori*. In order to perform further derivations, two relatively non-restrictive assumptions are formulated:

- *Assumption 1:* Sampling starts exactly at the beginning of the period of $u(t)$.
- *Assumption 2:* The ratio between the period of $u(t)$ and the sampling interval is a rational number.

Under the above assumptions and due to the nature of $\sin(\omega k\tau)$ it is easy to see that the experimental conditions are cyclically repeated. When some experiments are repeated then the number n_e of distinct experimental conditions is less than the total number of observations n_t . The design resulting from this approach is called a continuous experimental design (Atkinson and Donev, 1992; Uciński, 2005; Walter and Pronzato, 1997). FIM can then be written as:

$$\mathbf{P}^{-1} = \mathbf{P}_2 \sum_{k=1}^{n_e} \mu_k \mathbf{r}_{2,k} \mathbf{r}_{2,k}^T \mathbf{P}_2. \quad (23)$$

where $\mu_k = w_k/n_t$, w_k is the number of repetitions of measurements under the k -th experimental condition. Caratheodory's theorem then indicates that (23) can always be written with a linear combination of at most $n_e = n_p(n_p + 1)/2 + 1$ ($n_e = 4$ since we have two parameters R and C) matrices $\mathbf{r}_{2,k} \mathbf{r}_{2,k}^T$. In the sequel, the setting $n_e = 4$ is employed.

It can be shown that:

$$\det(\mathbf{P}^{-1}) = \det(\mathbf{P}_2)^2 \det\left(\sum_{k=1}^{n_e} \mu_k \mathbf{r}_{2,k} \mathbf{r}_{2,k}^T\right).$$

After some relatively easy but lengthy calculations it can be shown that:

$$\begin{aligned} \det\left(\sum_{k=1}^{n_e} \mu_k \mathbf{r}_{2,k} \mathbf{r}_{2,k}^T\right) &= \sin(\omega\tau)^2 (16\mu_1\mu_4 \cos(\omega\tau)^4 \\ &+ 4(\mu_1\mu_3 + \mu_2\mu_4 - 2\mu_1\mu_4) \cos(\omega\tau)^2 + \mu_1\mu_4 \\ &+ \mu_1\mu_2 + \mu_2\mu_3 + \mu_3\mu_4) \end{aligned} \quad (24)$$

It can easily be observed that (24) is independent of R , C and R_r . On the other hand, \mathbf{P}_2 does not depend on τ . This means that maximisation of FIM with respect to τ is equivalent to:

$$\tau^* = \arg \max_{\tau > 0, \mu_i, i=1, \dots, n_e} \det\left(\sum_{k=1}^{n_e} \mu_k \mathbf{r}_{2,k} \mathbf{r}_{2,k}^T\right). \quad (25)$$

While maximisation of FIM with respect to R_r is equivalent to

$$R_r^* = \arg \max_{R_r > 0} \det(\mathbf{P}_2) = \arg \max_{R_r > 0} 2\rho^2 \omega U^2 R^2 R_r^2. \quad (26)$$

The solution of (25) is given as follows:

$$\tau^* = \frac{\pi(1+i)}{2\omega}, \quad i = 0 \quad (27)$$

with $\mu_k = 1/4$, $k = 1, \dots, n_e = 4$. Note that i is equal zero which is equivalent to the sampling frequency two times larger than that of the input signal. While the D-optimum value of an auxiliary resistance R_r^* being the solution of (26) can be written according to:

$$R_r^* = \frac{R}{\sqrt{1 + \omega^2 R^2 C^2}}. \quad (28)$$

2.4 Other properties

The objective of this section is to investigate the influence of the experimental conditions (27) and (28) on the estimation accuracy of \mathbf{p} . First let us define FIM for \mathbf{p} :

$$\begin{aligned} \mathbf{P}^{-1} &= \sum_{k=1}^{n_t} \mathbf{r}_k \mathbf{r}_k^T, \mathbf{r}_k = \begin{bmatrix} \frac{\partial v_k}{\partial p_1} & \frac{\partial v_k}{\partial p_2} \end{bmatrix}^T \\ &= U\sqrt{2} [\sin(\omega\tau k), \cos(\omega\tau k)]^T, \end{aligned} \quad (29)$$

Thus, FIM for the continuous design can be written as:

$$\mathbf{P}^{-1} = \sum_{k=1}^{n_e=4} \mathbf{r}_k \mathbf{r}_k^T. \quad (30)$$

Substituting (27) into (30) it can be shown that:

$$\mathbf{P}^{-1} = 2U^2 \text{diag}(\mu_1 + \mu_3, \mu_2 + \mu_4). \quad (31)$$

From (31) it can be observed that FIM is diagonal. A design satisfying this property is called the *orthogonal design*. Its appealing property is that the covariance between the parameters p_1 and p_2 equals zero, which means that they are estimated independently. The remaining task is to check if the experimental conditions (27)–(28) are D-optimum for \mathbf{p} . In order to do that the following useful criterion can be used (Atkinson and Donev, 1992; Walter and Pronzato, 1997):

$$\mathbf{r}_k \mathbf{P} \mathbf{r}_k \leq n_p. \quad (32)$$

when the equality holds for \mathbf{r}_k satisfying the experimental conditions (27) and (28). Substituting $n_p = 2$ and then (31) into (32) it can be shown that:

$$\frac{\sin(\frac{1}{2}\pi k)^2}{\mu_1 + \mu_3} + \frac{\cos(\frac{1}{2}\pi k)^2}{\mu_1 + \mu_3} \leq 2. \quad (33)$$

Setting $\mu_k = 1/4$, $k = 1, \dots, n_e = 4$ in (33) implies that the experimental design (27)–(28) is D-optimum and orthogonal for \mathbf{p} .

3. EXPERIMENTAL RESULTS

Let us consider a numerical simulation example for the following parameters: $R = 500\text{Ohm}$, $C = 300\text{nF}$, $\omega = 1000\pi$, $\tau = \tau^*$ (for $i = 0$). For the purpose of simulation v_k was disturbed with noise generated according to the uniform distribution $\mathcal{U}(-3 \times 10^{-4}, 3 \times 10^{-4})$. Two different experiments

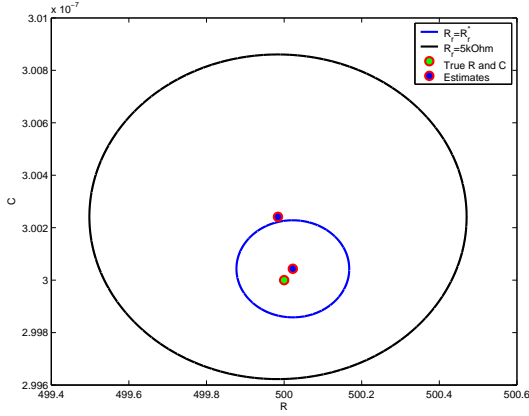


Fig. 2. The confidence region (16) for different R_r and the associated estimates

were performed for two different values of R_r , i.e. $R_r = R_r^*$ and $R_r = 5\text{k}\Omega$. Figure 2 presents the obtained confidence regions and the associated estimates of R and C (assuming $\alpha = 0.01$, i.e. 99% confidence region). From these results it is clear that the proposed solution provides more accurate estimates with considerably smaller uncertainty than those obtained without it. Undoubtedly, this will result in an increased fault sensitivity and in a general improvement of the reliability of the proposed fault detection scheme.

Let us assume that the non-faulty R and C are $R = 500.03[\Omega]$ and $C = 300.6[\text{nF}]$. Thus, the problem of fault detection boils down to the task of testing:

$$\begin{aligned} \mathcal{H}_0 : (R, C) &= (500.03[\Omega], 300.6[\text{nF}]) \\ \text{vs.} \\ \mathcal{H}_1 : (R, C) &\neq (500.03[\Omega], 300.6[\text{nF}]). \end{aligned} \quad (34)$$

It can be observed from Fig. 2 and inequality (16) that hypothesis \mathcal{H}_0 is rejected when $R_r = R_r^*$ which means that a fault occurs. Contrary, hypothesis \mathcal{H}_0 is accepted when $R_r = 5[\text{k}\Omega]$ which means that there is no fault. These results clearly indicate that the application of the D-optimum experimental conditions increases the fault sensitivity, i.e. it makes the proposed fault diagnosis scheme more reliable.

3.1 Accuracy analysis

The main objective of this section is to estimate the measurement accuracy provided by the considered approach. For that purpose a set of different impedances were selected (similar to that of (Angrisani *et al.*, 1996)). The relative measurement errors were defined as:

$$\delta_R = \frac{R - \hat{R}}{R} 100[\%], \quad \delta_C = \frac{C - \hat{C}}{C} 100[\%], \quad (35)$$

Each measurement was repeated 50 times and then the mean measured values \bar{R} and \bar{C} were

calculated and for each of them a coefficient of variation $\bar{\sigma}$ was computed:

$$\bar{\sigma} = \frac{\sigma_R}{\bar{R}} 100[\%], \quad \text{or} \quad \bar{\sigma} = \frac{\sigma_C}{\bar{C}} 100[\%], \quad (36)$$

where σ_C (or σ_R) stands for the standard deviation of 50 measurements. Table 1 shows the achieved results. From this results it is clear that the proposed approach provides a high measurement accuracy. It should be also pointed out that these measurements were achieved for $n_t = 4000$ which implies that the measurement time was 1[s]. Figure 3 shows the evolution of the relative

Table 1. Simulation results

	True value	Mean measured value	$\bar{\sigma}[\%]$
C	0.75[nF]	0.7502[nF]	0.41
R	500[Ω]	499.9997[Ω]	$9.2252 * 10^{-4}$
C	150[nF]	150[nF]	0.0018
R	570[Ω]	569.999[Ω]	$9.3179 * 10^{-4}$
C	320[nF]	320[nF]	$4.6464 * 10^{-4}$
R	48[kΩ]	4.7999[kΩ]	0.0425
C	1[nF]	0.9998[nF]	0.1441
R	1[kΩ]	999.99[Ω]	0.0010
C	50[nF]	50[nF]	0.0028
R	1.1[kΩ]	1.1[kΩ]	$8.7803 * 10^{-4}$
C	160[nF]	160[nF]	$5.1671 * 10^{-4}$
R	97[kΩ]	96.986[kΩ]	0.0391
C	840[pF]	840[pF]	0.0313
R	5[kΩ]	5[kΩ]	$8.6657 * 10^{-4}$
C	15[nF]	15[nF]	0.0018
R	5.7[kΩ]	5.7[kΩ]	$9.1961 * 10^{-4}$
C	32[nF]	32[nF]	$4.5223 * 10^{-4}$
R	296[kΩ]	296[kΩ]	0.0301
C	540[pF]	540[pF]	0.0220
R	10[kΩ]	10[kΩ]	$8.8802 * 10^{-4}$
C	13[nF]	13[nF]	$8.8790 * 10^{-4}$
R	17[kΩ]	17[kΩ]	0.0012
C	16[nF]	16[nF]	$5.3046 * 10^{-4}$
R	495[kΩ]	495.01[kΩ]	0.0245

errors (35) (for $R = 500[\Omega]$, $C = 0.75[\text{nF}]$, and $R_r = R_r^*$) in the consecutive iterations of the proposed algorithm. From these results it is clear that relatively high measurement accuracies can be achieved after a few hundred iterations only. This corresponds to the measurement time less than 0.25[s].

4. CONCLUSION

It was shown that the experimental conditions do not concern an appropriate input selection only but can also provide rules for selecting other parameters, e.g. sampling time, auxiliary resistances, etc. In particular, the problem of impedance measurement was transformed into the parameter estimation task. Contrary to the approaches presented in the literature, parameter estimation was realized with the use of the linear least-square method (or the recursive least-square method when an on-line measurement is

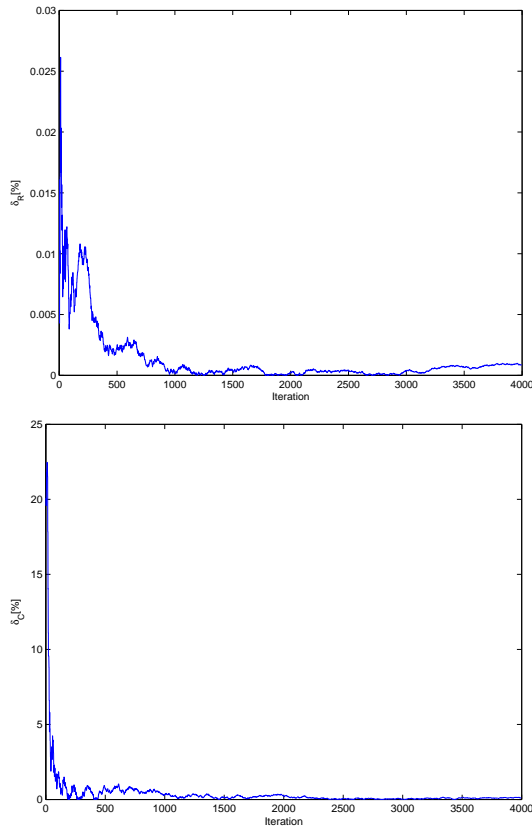


Fig. 3. Relative errors in the subsequent iterations of the proposed algorithm

required) which enables fast convergence rate. Another important contribution of this paper was the development of the D-optimum experimental conditions that make it possible to enhance the measurement accuracy. In particular, explicit formulae for selecting the reference resistance R_r and the sampling time τ were provided. It was also shown that the proposed approach can effectively be applied for fault detection which is very important from the point of view of modern control and fault diagnosis. The numerical experiments performed with the proposed impedance measurement scheme confirm that the application of OED is very profitable and leads to the decreased modelling uncertainty and an increased fault sensitivity.

ACKNOWLEDGMENTS

The work was supported by State Committee for Scientific Research in Poland (KBN) under the grant 4T11A01425 *Modelling and identification of non-linear dynamic systems in robust diagnostics.*

The author would like to express his sincere gratitude to the referees, whose efforts have significantly improved the paper's quality.

REFERENCES

- Angrisani L., Baccigalupi A., and Pietrosanto A. (1996): *A digital signal-processing instrument for impedance measurement.* – IEEE Instrum. Meas., Vol.45, No. 6 pp. 930–934.
- Atkinson A.C. and Donev A.N. (1992): *Optimum Experimental Designs.* – New York: Oxford University Press.
- Awad S.S., N. Narasimhamurthi, W.H. Ward (1994): *Analysis, design, and implementation of an AC bridge for impedance measurements.* – IEEE Instrum. Meas., Vol.36, pp. 894–897.
- Chen J. and Patton R. J. (1999): *Robust Model-based Fault Diagnosis for Dynamic Systems.* – London: Kluwer Academic Publishers.
- Delebecque F., Nikoukah R., and Rubio Scola H. (2003) *Test signal design for failure detection: A linear programming approach.* – Int. J. Appl. Math. Comput. Sci., Vol. 13, No. 4, pp. 515–526.
- Dutta M., Rakshid A., S.N. Battacharyya, and J.K. Choudhury (1987): *An application of the LMS adaptive algorithm for a digital AC bridge.* – IEEE Instrum. Meas., Vol.36, pp. 894–897.
- Frank P.M., Schreier G. and Garcia E.A. (1999): *Nonlinear observers for fault detection and isolation.* – In: New Directions in Nonlinear Observer Design (Nijmeijer H., Fossen T.I., Eds.) – Berlin: Springer-Verlag.
- Gupta M.M., Jin L. and Homma N. (2003): *Static and Dynamic Neural Networks. From Fundamentals to Advanced Theory.* – New Jersey: Wiley.
- Korbicz J., Kościelny J.M., Kowalczyk Z. and Cholewa W. (Eds.) (2004): *Fault Diagnosis. Models, Artificial Intelligence, Applications.* – Berlin: Springer-Verlag.
- Uciński D. (2005) *Optimal measurements methods for distributed parameter system identification.* – New York: CRC Press.
- Walter E. and Pronzato L. (1997): *Identification of Parametric Models from Experimental Data.* – London: Springer.
- Witczak M. (2003): *Identification and Fault Detection of Non-linear Dynamic Systems.* – Zielona Góra: University of Zielona Góra Press.